Novel-Graphene-Nanoelectrodes-Based Terahertz Photomixers

A. J. Jumaah,[1] J. M. B. P. Sosa,[1] I. T. Monroy,[1] J. Gómez Rivas Rivas,[2] H. G. Roskos,[3] and S. Al-Daffaie[1]

[1] Department of Electrical Engineering, Eindhoven University of Technology
[2] Department of Applied Physics and Science Education, Eindhoven University of Technology
[3] Physikalisches Institut, Goethe-Universität Frankfurt am Main

Abstract

Novel Terahertz (THz) photomixers fabricated on low-temperature-grown (LTG) GaAs are demonstrated using multi-layer-graphene (MLG) as transparent nanoelectrodes instead of conventional opaque metal electrodes. MLG improves sensitivity and responsivity by more than one order of magnitude. The higher responsivity of the new interdigitated graphene device leads to an enormously enhanced dynamic range. Also the bandwidth of the new THz MLG-based photodetector is increased twice as compared with the metallic interdigitated THz photodetector devices. The main enhancements of graphene finger nanoelectrodes are due to the transparency of the graphene. That was approved by simulations, where more than 97% of the light beam allows propagating through graphene for excitation. The area under the graphene fingers is fully exposed to light added to the edges, whereas only the edges are covered by light in conventional devices. Therefore, the graphene electrodes result in higher photocarriers that are modulated by the incoming THz wave and enhance the responsivity of the device. The functionality of the MLG does not depend on the incident laser wavelength and the active photoconductive materials. There is no reason to assume that this benefit of graphene nanoelectrodes is limited to LTG-GaAs-based photomixer devices. We expect similar responsivity enhancements for other photomixing materials, as they are used, e.g., in the 1.3-1.55 μm wavelength regime of fiber-based telecommunication.

Introduction

Graphene, consisting of a 2D monolayer of carbon atoms arranged in a hexagonal lattice, is one of the most attractive materials being investigated due to its unique optical and electrical properties. Graphene absorbs only 2.3% of visible light [1]. The gapless electronic band structure and high intrinsic mobility of graphene make it a highly desirable material to substitute metals as electrical conductors, provided the Fermi level is high. The combination of high transparency and conductivity makes the graphene a very attractive material as transparent conductive electrode for optoelectronic devices [2]. This pertains also to THz photoconductor devices (THz photomixers). Photoconductor devices are of particular interest in the THz research field, since they can act as THz emitters and detectors, especially if a wide range of tunability of terahertz devices is required. For the generation of the continuous-wave (CW) THz signals, two single-frequency, but frequency-tunable optical waves are mixed in a high-speed photoconductive material. The waves are in-coupled through metallic electrodes of an electrically biased broadband antenna [3]. The generated photocurrent depends on the incident optical power and oscillates with a frequency corresponding to the frequency difference of the two optical waves, which is chosen to be in the THz region. The higher the optical power, which reaches the photoconductive materials, the higher the generated

photocurrent which can be obtained, and the higher the THz output power will become [4]. The oscillation frequency of the generated photocurrent can easily be adjusted over the full bandwidth of the photoconductive antenna by tuning the frequency difference of the two optical waves [5]. It has recently been shown that THz interdigitated graphene photoconductor devices are far superior to standard ones with metallic electrodes. In Refs. [6-9], it has been shown that the charge carriers excited directly under the transparent graphene nanoelectrodes contribute enormously to the generated photocurrent which leads to a substantial increase in the THz output power [10, 11].

A significant advantage of photoconductor devices is that they can also be used as THz detectors [12, 13]. In this detector approach, the device operates without an external bias field. The incoming optical beatnote modulates the carrier density and thus the conductance of the semiconductor between the antenna leaves (which together represent a photoconductive antenna). The electric radiation field of the THz wave will act as a bias field and accelerate the photogenerated carriers. The product of the optical beat signal and the THz field results in a photocurrent that is dependent on the amplitude of the incident THz wave and the phase difference between that wave and the optical beatnote. In CW homodyne measurement systems, as shown schematically in Figure 1, two photoconductor devices are implemented. The first photoconductor (emitter) is used to generate THz waves. The second photoconductor (receiver) is used to detect the generated THz waves. In these CW homodyne measurement systems, the optical beat signal is split into two paths. The first path is used for the THz source, where the device needs a bias field to generate THz waves. Optical components, such as lenses and parabolic mirrors, are used to align and focus the THz beam onto the photoconductor receiver. The second path is used for the THz detector.

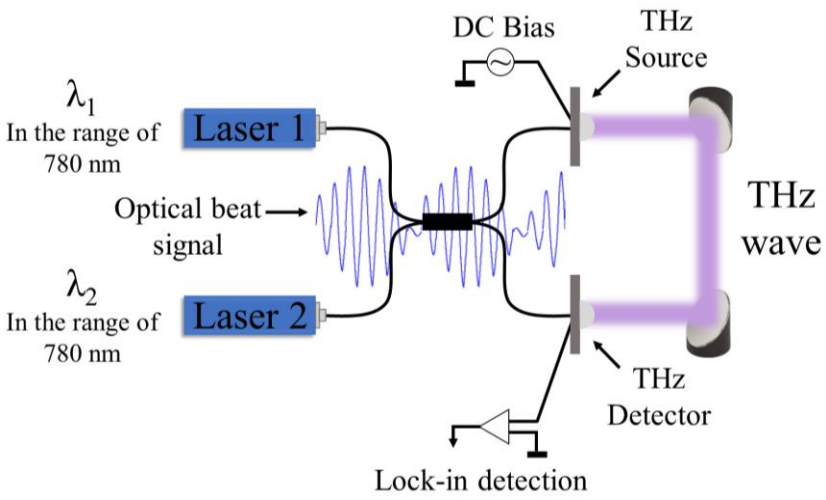

Figure 1: Coherent detection with a CW THz measurement system

Graphene Transparency

When an incident optical beat signal is projected onto the active area of a photoconductor device, free carriers are generated inside the photoconductive material [13]. The THz wave is usually injected through the substrate and hits the photoconductive antenna from the opposite side. The electric field of the incoming THz wave acts as a bias field that generates a voltage drop V_{THz} between the antenna contacts. Combined with the modulation of the conductivity by the optical beat signal, the detected photocurrent is

$$I_{det} = V_{THz}G = e\mu_c n_c V_{THz}\frac{A}{l} \quad (1)$$

where G is the device conductance, e the electron charge, μ_c the carrier mobility, n_c the carrier concentration, A the electrodes area, and l the length of the propagation path which the generated photocarriers follow to reach the electrode. The higher the optical power which reaches the photoconductive material, the higher the generated density of photocarriers, and the higher the measured photocurrent which determines the detector sensitivity. In conventional photomixers with metallic finger electrodes, these will reflect the light beam. The light will excite charge carriers only in the gap between the electrode fingers. Of these carriers, only those generated close to the edges of the electrodes finally contribute to the photocurrent because of the ultrashort lifetime of the charge carriers in the semiconductor. In contrast, graphene electrodes allow the optical beat signal to excite also the area under the electrodes. Many more charge carriers then contribute to the measured photocurrent [14], which leads to a pronounced increase in the sensitivity of the THz photoconductor detector [14, 15, 16].

Device Fabrication

The new interdigitated graphene detector was fabricated by transferring 6-8 layers of CVD-grown graphene onto the top of a low-temperature growth (LTG) GaAs substrate. The LTG-GaAs layer (wafer thickness ~ 1.5 µm) was grown on top of a GaAs substrate. A broadband spiral antenna with 10 µm separation between the antenna contacts was fabricated on the graphene sheet using a standard optical lithography process. A second optical lithography process and an etching of the MLG in an oxygen plasma were performed to form the interdigitated configuration of the MLG. The interdigitated configuration was performed with a finger width of 0.5 µm, a spacing gap between the fingers of 1.5 µm, and the finger length of 9 µm, as shown in Figure 2a. A layer of SiNx of 150 nm coats the device to isolate the graphene nanoelectrodes from environmental contamination. In addition, detectors with interdigitated gold fingers were fabricated in a single photolithographic lift-off process including a 150 nm thick Au layer on LTG-GaAs. The same fingers configuration was performed for the metallic electrodes of the detectors, as shown in Figure 2b.

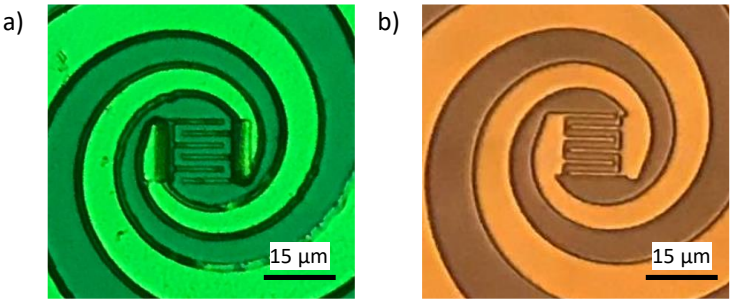

Figure 2: CW THz detectors with: a) interdigitated MLG electrodes, and b) interdigitated gold electrodes.

THz Measurements

The sensitivity of the new THz interdigitated graphene photoconductor detector was compared experimentally with the performance of a standard photoconductor detector

using a commercial THz source. For this purpose, the commercial THz source was set in a homodyne coherent detection configuration. The interdigitated graphene photoconductor detector had the same geometrical dimensions of the interdigitated graphene electrodes as the standard metal-finger-based photoconductor device. Two detuned distributed feedback diode lasers (DFB-LDs) (λ = 780 nm) were used to characterize the two detectors in a homodyne detection system. Total optical powers of 31 mW and 30.5 mW were used to illuminate the active areas of the emitter and the detector photoconductor, respectively. The frequency difference between the two detuned DFB-LDs was controlled by temperature and current controllers. The frequency of the THz radiation from the THz emitter was tuned by varying the frequency difference between the two DFB-LDs. A scanning range of the THz radiation from 50 GHz to 1.9 THz was obtained, allowing us to measure the frequency-dependent photocurrent for both photoconductor devices over a large frequency range.

Results and Discussion

A frequency step of 50 MHz was chosen to scan the THz radiation from 50 GHz to 1.9 THz. Figure 3 shows the detected THz photocurrent for the interdigitated graphene photoconductor device. This photocurrent is compared with the reference data obtained using the conventional metal-electrodes-based photoconductor device. For both devices, the photocurrent exhibits a peak in the 100-GHz range, followed by a gradual roll-off to the noise floor. The roll-off is mainly determined by the frequency characteristics of the emitter and detector antennas together with the lifetime of the charge carriers. The most important feature of the measurements is, however, that the graphene photoconductor exhibits a more than one order of magnitude (20 times) larger photocurrent than the standard metal-finger-based device, and this over the whole frequency range with a measureable photocurrent. Furthermore, the interdigitated graphene photoconductor device was able to detect the THz beam up to 1.25 THz, which is twice the bandwidth of the standard metal-finger-based device. This enhancement in the device performance is attributed to the high conductivity and high transparency of graphene, which allows almost all of the light beam to penetrate the nanoelectrode material and increase the number of carriers which contribute to the photocurrent.

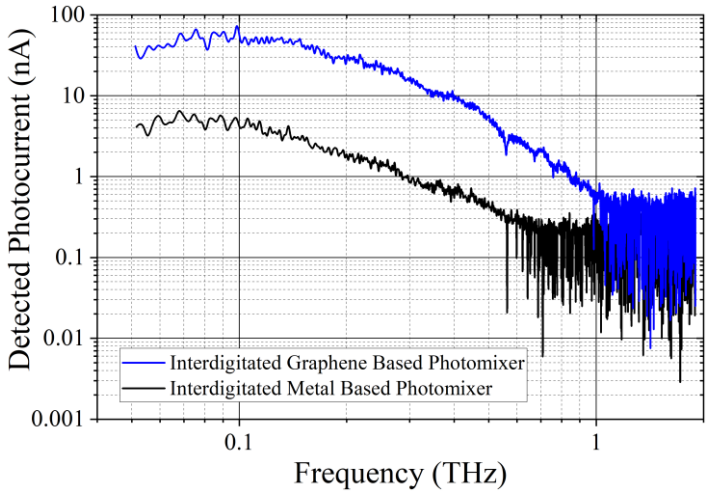

Figure 3: Comparison of the detected THz photocurrent of the detector with interdigitated graphene electrodes with that of the detector with metal electrodes.

Conclusions

The work presented here demonstrates room-temperature coherent detection of CW THz radiation using a new type of THz photoconductor device based on interdigitated graphene nanoelectrodes on LTG-GaAs photoconductive material. The device was compared with a standard metal-finger-based photoconductor device. The high optical transparency of graphene allows most of the optical light beam to penetrate the graphene nanoelectrodes of the fingers. The higher the transmitted light intensity, the higher the photogenerated carrier density, and the higher the detected photocurrent. The measurements show a more than one order of magnitude increase of the detected photocurrent compared to the standard metal-finger-based photoconductor device. Additionally, the interdigitated graphene detector exhibits a bandwidth twice as large as that of the standard metal-finger-based detector. This performance of the graphene nanoelectrodes offers a new path to provide highly responsive devices for THz applications.

References

[1] P. Li, C. Chen, J. Zhang, S. Li, B. Sun, and Q. Bao, "Graphene-based transparent electrodes for hybrid solar cells," Front. materials vol. 1, 26, 2014.

[2] Y. Jiang, L. Gao, X. Wang, W. Dai, J. Wu, X. Dai, and G. Zou, "Laser tailored multilayer graphene grids for transparent conductive electrodes," Nanoscale research letters, vol. 14, 1–6, 2019.

[3] K.A. McIntosh, E. R. Brown, K. B. Nichols, O. B. McMahon, W. F. DiNatale, and T. M. Lyszczarz, "Terahertz photomixing with diode lasers in low-temperature-grown GaAs," Applied Physics Letters vol. 67, no. 26, 3844-3846, 1995.

[4] S. Al-Daffaie, O. Yilmazoglu, F. Küppers, and H. L. Hartnagel. "1-D and 2-D nanocontacts for reliable and efficient terahertz photomixers," IEEE Transactions on Terahertz Science and Technology vol. 5, no. 3, 398-405, 2015.

[5] R. Mendis, C. Sydlo, J. Sigmund, M. Feiginov, P. Meissner, and H.L. Hartnagel, "Tunable CW-THz system with a log-periodic photoconductive emitter," Solid-State Electronics, vol. 48, no. 10-11, 2041-2045, 2004.

[6] A. Jumaah, S. Al-Daffaie, O. Yilmazoglu, and F. Küppers, "Graphene–nanowire hybrid photomixer for continuous-wave terahertz generation," in 42nd International Conference on Infrared, Millimeter, and Terahertz Waves (IRMMW-THz). IEEE, 1-2, 2017.

[7] A. Jumaah, S. Al-Daffaie, O. Yilmazoglu, F. Küppers, and T. Kusserow, "Interdigital multilayer-graphene nanoelectrodes for continuous wave terahertz photomixers," in European Microwave Conference in Central Europe (EuMCE), IEEE, 265-267, 2019.

[8] A. Jumaah, S. Al-Daffaie, O. Yilmazoglu, F. Küppers, and T. Kusserow, "Experimental investigation of graphene layers as 2d nanoelectrodes for continuous wave terahertz generation," in 44th International Conference on Infrared, Millimeter, and Terahertz Waves (IRMMW-THz), IEEE, 1-2, 2019.

[9] A. J. Jumaah, S. Al-Daffaie, T. Kusserow, I.T. Monroy, "Highly transparent graphene electrodes for cw thz applications, In 45th International Conference on Infrared, Millimeter, and Terahertz Waves (IRMMW-THz), IEEE 1–2, 2020.

[10] A. J. Jumaah, S. Al-Daffaie, O. Yilmazoglu, and T. Kusserow, "Continuous-wave terahertz emitter with hybrid nanoelectrodes based on graphene and nanowire," OSA continuum vol. 3, no. 7, 1826-1833, 2020.

[11] A. Jumaah, S. Al-Daffaie, O. Yilmazoglu, and F. Küppers, "Graphene enhanced 2-D nanoelectrode for continuous wave terahertz photomixers," In 43rd International Conference on Infrared, Millimeter, and Terahertz Waves (IRMMW-THz), IEEE, 1-2, 2018.

[12] F. Sizov, and A. Rogalski, "THz detectors", Progress in Quantum Electronics, vol. 34, no. 5, 278-347, 2010.

[13] A. J. Jumaah, S. Al-Daffaie, T. Kusserow, and I.T. Monroy. "High performance graphene-based CW THz photoconductive detector," In 45th International Conference on Infrared, Millimeter, and Terahertz Waves (IRMMW-THz), IEEE, 01-02, 2020.

[14] A. J. Jumaah, H. G. Roskos, and S. Al-Daffaie, "Novel-coupled graphene nanoelectrodes enhanced terahertz photodetector," APL Photonics, [Under review].

[15] A. Rogalski, “Terahertz detectors and focal plane arrays,” Elektronika: konstrukcje, technologie, zastosowania, vol. 51, no. 4, 93-108, 2010.
[16] E. Moreno, Z. Hemmat, J. B. Roldán, M. F. Pantoja, A. R. Bretones, and S. G. García, “Time-domain numerical modeling of terahertz receivers based on photoconductive antennas,” JOSA B, vol. 32, no. 10, 2034-2041, 2015.